

Inducing plasmonic exceptional points and pattern formation with modulated Floquet parametric driving

Egor I. Kiselev,¹ Mark S. Rudner,^{2,3} and Netanel H. Lindner¹

¹*Physics Department, Technion, 320003 Haifa, Israel*

²*Department of Physics, University of Washington, Seattle, Washington 98195-1560, USA*

³*Niels Bohr Institute, University of Copenhagen, 2100 Copenhagen, Denmark*

We propose a method to parametrically excite low frequency collective modes in an interacting many body system using a Floquet driving at optical frequencies with a modulated amplitude. We demonstrate that it can be used to design plasmonic time-varying media with singular dispersions. Plasmons near resonance with half the modulation frequency exhibit two lines of exceptional points connected by dispersionless states. Above a critical driving strength, resonant plasmon modes become unstable and arrange themselves in a crystal-like structure stabilized by interactions and nonlinearities. This new state breaks the discrete time translational symmetry of the drive as well as the translational and rotational spatial symmetries of the system and exhibits soft, Goldstone-like phononic excitations.

I. INTRODUCTION

The collective modes of a many-body system fingerprint the symmetries underlying a phase of matter. They also play an important role in transitions to non-equilibrium states when the system is subjected to an external drive. Resonantly driving collective modes can lead to exotic wave propagation effects and, at strong driving, to instabilities leading to new symmetry breaking non-equilibrium states [1–5]. An example for such an instability in classical physics are Faraday waves formed by parametrically driven surface waves [6–8].

Accessing this type of phenomena in electronic systems is challenging due to a lack of methods for the control and manipulation of collective modes in solids. At the same time, the possibility holds a lot of promise for applications in fields like plasmonics or spintronics. Here, we show that Floquet engineering, which employs driving at optical frequencies to manipulate electronic bandstructures [9–38], can be an effective tool to control collective modes. In particular, we show that off-resonant driving fields can parametrically couple to plasmon modes via a mechanism we call “modulated Floquet parametric driving” (MFPD), leading to the formation of exceptional points and non-dispersive plasmonic states. For strong driving, we predict the existence of an emergent non-equilibrium state with spatio-temporal correlations that break time and space translation symmetry.

MFPD takes advantage of the fact that the electronic properties of two dimensional materials are modified in the presence of a high frequency time-periodic driving fields [39]. Changing the parameters of these fields, an electronic system can be controlled dynamically. As illustrated in Fig.1 a), a high-frequency Floquet driving alters the shape of the quasi-energy bands (red curves). In particular, the effective mass m^* of electrons at the Fermi surface changes. This change results in an altered plasmon dispersion. A periodic modulation of the Floquet drive’s amplitude results in a periodically changing mass that parametrically excites plasmon modes. This

effect induces two lines of exceptional points in the plasmon dispersion (Fig.1 b)). These exceptional lines are separated by a non-dispersive gap with localized plasmon modes.-

For sufficiently strong driving, plasmons with wavenumbers q^* meeting the condition $\omega_{\text{pl}}(q^*) = \omega_1$, where $\omega_{\text{pl}}(q)$ is the plasmon dispersion and $2\omega_1$ is the amplitude modulation frequency, become unstable and, after a short period of exponential growth, form a crystal-like lattice with a periodically modulated electron density (Fig.1 c)). The structure of this crystal is determined by the nonlinearities of the system. The density oscillates at half the modulation frequency, thus breaking the π/ω_1 discrete time translation symmetry of the drive – a behavior known from discrete time crystals [40–45].

An important challenge in Floquet engineered systems is heating [46–60]. Here, we show that the parametric excitation of plasmons by MFPD can be achieved in an off-resonant regime where (momentum conserving) single-photon excitation of electrons is blocked. To achieve this, the drive Frequency Ω_F and the Fermi energy μ must be chosen such that all electronic states supporting a resonant interband single photon excitation with an energy transfer of $\hbar\Omega_F$ and near-zero momentum transfer lie below the Fermi surface (see Fig. 1). Processes involving multiple photons are suppressed in the ratio of drive amplitude and drive frequency, leading to strongly reduced heating rates due to photoexcited electrons.

Below, we describe in more detail the the creation of singular plasmon dispersions and the excitation of plasmonic instabilities by MFPD, the transition into the crystalline state and the propagation of Goldstone-like, phononic collective modes in the symmetry broken state.

II. EQUATIONS OF MOTION FOR COLLECTIVE DYNAMICS

To describe the electron dynamics, the onset of instability, and the transition to the broken symmetry state,

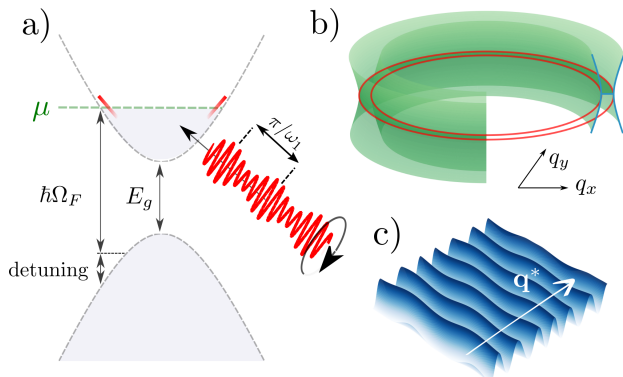


Figure 1. Modulated Floquet parametric driving, exceptional lines and non-equilibrium steady states: a) Illustration of the quasi-energy bands of electrons in a gapped system under MFPD. The dashed gray lines represent the undriven band structure. A Floquet signal with the frequency Ω_F , where $\hbar\Omega_F > E_g$, is applied. The quasi-energy bands in the vicinity of the Fermi surface for a non-zero driving amplitude are shown in red. By modulating the amplitude of the fast Floquet drive with a frequency $2\omega_1$, an oscillation of the dispersion and the effective mass of the electrons at the Fermi level is induced (see Eq. (10)). b) The periodic modulation of the Fermi velocity induces two lines of exceptional points (shown as red circles) in the rotationally symmetric dispersion of the soft THz plasmon mode (green surfaces) – see Fig. 2 for an in-detail cross-sectional view. c) Above a critical value, the mass oscillation parametrically excites THz plasmons. Due to nonlinear and interaction effects, the plasmons arrange themselves in a crystal-like structure (shown in blue) whose periodicity is determined by the condition $\omega_1 = \omega_{\text{pl}}(q^*)$, where $\omega_{\text{pl}}(q)$ is the plasmon dispersion. The crystalline state breaks the rotational and translational symmetries of the undriven system and supports soft phonon-like Goldstone modes which are shown in the figure as small deviations from the plane wave structure of the plasmon lattice.

we use a hydrodynamic description of Coulomb interacting electrons (see e.g. [61–63]). The equations of motion follow from the conservation of charge and momentum [64–66]. The continuity equation for the electron density ρ is

$$\partial_t \rho(t, \mathbf{x}) = -\partial_i \rho(t, \mathbf{x}) u_i(t, \mathbf{x}), \quad (1)$$

where $\mathbf{u}(t, \mathbf{x})$ is the electron flow velocity. The continuity equation for the momentum density is given by the Euler equation

$$\partial_t m^* \rho u_i + \partial_j \Pi_{ij} = -\gamma m^* \rho u_i - e \rho \partial_i \phi, \quad (2)$$

where $m^* = \hbar k_F / v_F$ is the effective mass of electrons at the Fermi surface given by the ratio of Fermi momentum $\hbar k_F$ and Fermi velocity v_F , u_i is the electron flow velocity, and γ is the rate of momentum relaxation, e.g. due to impurity or phonon scattering. The stress tensor Π_{ij} is given by

$$\Pi_{ij} = m^* \rho u_i u_j + \delta_{ij} p, \quad (3)$$

where p is the pressure. The electrostatic potential is given by

$$\phi(t, \mathbf{x}) = \int d^2 x' \frac{e \rho(t, \mathbf{x}')}{\varepsilon |\mathbf{x} - \mathbf{x}'|}. \quad (4)$$

Here e is the electron charge and ε the dielectric constant. Solutions of equations (1) and (2) describe the collective oscillations of the electron fluid. In the next section, we discuss how periodic driving can be used to modify the value of the electron mass m^* in these equations, and to realize MFPD.

III. MODULATED FLOQUET PARAMETRIC DRIVING AND CRYSTALLIZATION

A. Modulated Floquet parametric driving

The idea of MFPD is to use the dependence of the quasi-energy band structure on the parameters of the drive to couple to the soft collective modes of the system. Here, we show how the slow modulation of the driving amplitude leads to a time-varying effective electron mass. For concreteness, let us consider a coherently driven, gapped 2D Dirac system described by the Hamiltonian

$$H = \sum_{\mathbf{k}} \mathbf{c}_{\mathbf{k}}^\dagger [H_0(\mathbf{k}) + H_d(t)] \mathbf{c}_{\mathbf{k}} + \sum_{\mathbf{q}} V(\mathbf{q}) \hat{\rho}_{\mathbf{q}} \hat{\rho}_{-\mathbf{q}}. \quad (5)$$

We consider how the external drive modifies the dispersion in a single valley. The dispersion in the opposite valley is modified similarly. Both valley will be taken into account when considering the collective modes. For small values of \mathbf{k} around the center of the valley, we have $H_0 = \mathbf{d} \cdot \boldsymbol{\sigma}$, where $\mathbf{d} = [\lambda k_x, \lambda k_y, E_g/2]$ and $\boldsymbol{\sigma}$ is a Pauli matrix vector describing the orbital pseudospin degree of freedom. E_g is the energy gap between the two bands, $\mathbf{c}_{\mathbf{k}}^\dagger (\mathbf{c}_{\mathbf{k}})$ are electron creation (annihilation) operators and $H_d(t) = e \mathbf{A}(t) \cdot \nabla_{\mathbf{k}} H_0$ is the driving Hamiltonian derived from minimal coupling.

We assume circularly polarized light with an amplitude \mathcal{E} described by $\mathbf{A}(t) = (\mathcal{E}/\Omega) [-\sin \Omega_F t, \cos \Omega_F t, 0]$. The 2D Fourier transform of the Coulomb potential is given by $V(\mathbf{q}) = 2\pi/q$ and $\hat{\rho}_{\mathbf{q}} = \sum_{\mathbf{k}} \mathbf{c}_{\mathbf{k}}^\dagger \mathbf{c}_{\mathbf{k}+\mathbf{q}}$ is the density operator. We emphasize that we use the gapped Dirac Hamiltonian of Eq. (5) as an example. The physics presented here does not depend on the precise band structure of the system.

It is convenient to work in a rotating frame defined by the unitary transformation $U(t) = e^{i\mathbf{d} \cdot \boldsymbol{\sigma} \Omega_F t/2}$, where the spectrum of the transformed single-particle part of Eq. (5) is given by

$$\varepsilon_{\mathbf{k}} \approx \sqrt{\left(|\mathbf{d}| - \hbar \frac{\Omega_F}{2}\right)^2 + \frac{e^2 \mathcal{E}^2 \lambda^2}{4\Omega^2 \hbar^2} \left(2 - \frac{E_g}{|\mathbf{d}|}\right)} \quad (6)$$

for $\lambda k/|\mathbf{d}| \ll 1$, we neglected time dependent terms in the rotating frame [11]. In this frame and with the made approximations, the time dependence caused by the fast Ω_F oscillation of the Floquet drive does not explicitly appear in the equations.

We consider the metallic regime with the Fermi surface lying in the upper band (see Fig. 1) and expand the spectrum around k_F – the Fermi momentum of the undriven system. We write:

$$\varepsilon_k \approx \hbar v_F (\mathcal{E}, \Omega_F) (k - k_F) + \varepsilon_{k_F} (\mathcal{E}, \Omega_F) \quad (7)$$

The Fermi velocity $v_F (\mathcal{E}, \Omega_F)$ depends on the amplitude and frequency of the Floquet drive.

A variation of the drive amplitude \mathcal{E} results in a small change of the dispersion $\varepsilon_k \rightarrow \bar{\varepsilon}_k + \delta\varepsilon_k$ near the Fermi surface. To clearly distinguish between constant quantities and quantities oscillating with the slow modulation frequency ω_1 , here and in the following, we write the constant part with a bar. The total charge of the system is conserved and therefore k_F is fixed, however, the slope of ε_k at k_F and therefore the effective mass of the electrons $m^* = \hbar k_F / v_F (\mathcal{E}, \Omega_F)$ are altered. For a small $\delta\varepsilon_k$, we find

$$\bar{\varepsilon}_k + \delta\varepsilon_k \approx \left(1 - \frac{\delta m^*}{\bar{m}^*}\right) \frac{\hbar^2 k_F}{\bar{m}^*} (k - k_F). \quad (8)$$

We consider a slow, adiabatic oscillation of the electric field amplitude \mathcal{E} ,

$$\mathcal{E} (t) = \bar{\mathcal{E}} + \delta\mathcal{E} \cos (2\omega_1 t), \quad (9)$$

such that $\omega_1 \ll \Omega_F$. This slow oscillation does not couple to any single-electron degrees of freedom. However, as demonstrated below, it does couple to the soft plasmon mode through a parametric resonance induced by the periodic change of the effective mass

$$m^* (t) = \bar{m}^* \left(1 + \frac{\delta m^* (t)}{\bar{m}^*}\right). \quad (10)$$

B. Exceptional points and instability

The oscillating mass increment $\delta m^* (t)$ in Eq. (2) acts as a parametric drive, which is known to lead to instabilities [67]. In the following we identify the parametric instability of the charge density ρ . It is convenient to take the divergence of Eq. (2) and to combine the result with the continuity equation (1), including the drive-induced temporal modulation of $m^* (t)$. We find

$$\partial_t m^* (t) \partial_t \rho + \gamma m^* (t) \partial_t \rho - m^* (t) \partial_i \partial_j \rho u_i u_j = \partial_i \rho \partial_i \phi, \quad (11)$$

where we neglected the pressure term p in Eq. (11) since it's contribution is subleading to the long-range Coulomb potential [68, 69], [70]. Except otherwise indicated, here and in the following, derivatives act on all functions to the right. In what follows, we will also neglect the time

dependent contribution to the damping term, which is negligible in comparison to the static one.

We proceed with the linear stability analysis of Eq. (11). Writing $\rho = \bar{\rho} + \delta\rho$, where $\delta\rho$ is a small perturbation of the background charge density $\bar{\rho}$, and performing a Fourier transform in the spatial variables, to linear order in $\delta\rho$ we obtain

$$\partial_t (1 + h \cos (2\omega_1 t)) \partial_t \delta\rho_q + \gamma \partial_t \delta\rho_q + \omega_{\text{pl}}^2 (q) \delta\rho_q = 0, \quad (12)$$

where we have abbreviated $\delta m^* (t) / \bar{m}^* = h \cos (2\omega_1 t)$ and where $\omega_{\text{pl}} (q)$ is the plasmon dispersion

$$\omega_{\text{pl}} (q) = \sqrt{\frac{2\pi e^2 \bar{\rho} q}{\varepsilon \bar{m}^*}}. \quad (13)$$

Exponentially growing solutions for $\delta\rho_q$, with a growth rate proportional to the dimensionless mass modulation amplitude h , indicate unstable modes. Notice that Eq. (12) is equivalent to the equation describing the propagation of the magnetic field in photonic time crystals [71].

We first solve Eq. (12) in the vicinity of the resonance $\omega_{\text{pl}} (q) = \omega_1$ with the slowly varying envelope approximation [67]. We will then consider how the driving modifies the plasmon dispersion away from the resonance. The ansatz

$$\delta\rho_q = a_q (t) \cos (\omega_1 t) + b_q (t) \sin (\omega_1 t), \quad (14)$$

when used in Eq. (12), leads to the two equations

$$\begin{aligned} -\frac{1}{2}\omega_1^2 \hbar b_q - 2\dot{a}_q \omega_1 - \gamma a_q \omega_1 + (\omega_{\text{pl}}^2 (q) - \omega_1^2) b_q &= 0 \\ \frac{1}{2}\omega_1^2 \hbar a_q + 2\dot{b}_q \omega_1 + \gamma b_q \omega_1 + (\omega_{\text{pl}}^2 (q) - \omega_1^2) a_q &= 0, \end{aligned} \quad (15)$$

where we neglected the second derivatives of a_q and b_q , as they are of higher order in the small h around $\omega_{\text{pl}} (q) = \omega_1$. Assuming $a = a(0) e^{s(q)t}$, $b = b(0) e^{s(q)t}$, we find

$$s_{\pm} (q) = -\frac{\gamma}{2} \pm \frac{\omega_1}{2} \sqrt{\left(\frac{\hbar}{2}\right)^2 - \frac{(\omega_{\text{pl}}^2 (q) - \omega_1^2)^2}{\omega_1^4}}. \quad (16)$$

Exceptional points appear at wavenumbers q_{exc} , where the \pm -branches of $s_{\pm} (q)$ merge, i.e., when the condition $\omega_{\text{pl}}^2 (q_{\text{exc}}) = \omega_1^2 - \hbar/2$ is met. This results in a diverging group velocity $\partial s_{\pm} (q) / \partial q \sim |q - q_{\text{exc}}|^{-1/2}$ for $q \rightarrow q_{\text{exc}}$. In the interval between the two exceptional points q_{exc} , $s_{\pm} (q)$ is purely real. This corresponds to non-dispersive localized plasmons (see Fig. 2).

The instability condition $\text{Re}(s) > 0$ is realized for $h > 2\gamma/\omega_1$ in a narrow frequency range around $\omega_{\text{pl}} (q) = \omega_1$ given by

$$(\omega_{\text{pl}}^2 (q) - \omega_1^2)^2 < \omega_1^4 \hbar^2 / 4 - \omega_1^2 \gamma^2. \quad (17)$$

The fastest growing modes have wavenumbers q^* , which are determined by the condition

$$\pm\omega_{\text{pl}}(q^*) = \omega_1. \quad (18)$$

Thus, the parametric driving will excite plasmons with the frequency ω_1 , whose amplitude will grow according to $\delta\rho_{q^*} \sim e^{(h\omega_1/4 - \gamma/2)t}$. Notice that the system's response breaks the discrete time symmetry of the drive with respect to translations by $T = \pi/\omega_1$.

To obtain the full plasmon dispersion in the presence of parametric driving it is convenient to rewrite Eq. (14). According to Floquet's theorem, any solution to Eq. (12) can be written in the form $\delta\rho_q = e^{i\Lambda(q)t}u_\Lambda(t)$, where $u_\Lambda(t + \pi/\omega_1) = u_\Lambda(t)$. Comparing this form of the solution with the one in Eq. (14), we obtain the correspondence between $\Lambda(q)$ and $s(q)$:

$$\Lambda_\pm(q) = -is_\pm(q) + i\omega_1. \quad (19)$$

The function u_Λ is given by $u_\Lambda(t) = [a_\Lambda(0)(1 + e^{-2i\omega_1 t}) - ib_\Lambda(0)(1 - e^{-2i\omega_1 t})]/2$. Note, that the Floquet exponent $\Lambda(q)$ is defined modulo $2\omega_1$. In terms of the Bloch theory of electronic band structure, $2\omega_1$ plays the role of a reciprocal lattice vector. Eq. (19) is valid near $\omega_{\text{pl}}(q) = \omega_1$. For small q , keeping higher order derivatives in Eq. (15), and neglecting damping, we find that the two branches of the plasmon dispersion are given by $\Lambda_-(q) \approx 2i\omega_1 - i\omega_{\text{pl}}(q)/\sqrt{1+h^2/4}$ and $\Lambda_+(q) \approx i\omega_{\text{pl}}(q)/\sqrt{1+h^2/4}$. For Λ_- , we find $b_{\Lambda(q=0)} = -ia_{\Lambda(q=0)}$, giving $\delta\rho_q \approx a_{\Lambda(q)}e^{-i\omega_{\text{pl}}(q)t/\sqrt{1+h^2/4}}$. Therefore, the Λ_- branch is equivalent to a counter-propagating mode with the frequency $-i\omega_{\text{pl}}(q)/\sqrt{1+h^2/4}$ lifted by one reciprocal lattice vector $2\omega_1$.

Furthermore, the periodic driving opens a vertical non-dispersive gap around q^* , where the two branches of the plasmon dispersion meet. Inside the gap, the real part of $\Lambda_\pm(q)$ is flat. This phenomenon is known from photonic time varying media and photonic time crystals, where it is often referred to as momentum-gap or k-gap [71, 72]. In fact, Eq. (12) maps on the equation describing the propagation of light through a photonic time crystal [71]. The full plasmon dispersion near the onset of the instability ($h\omega_1/4 \gtrsim \gamma/2$) is illustrated in Fig.2.

C. Crystallization

Having identified the wavenumber q^* of the unstable modes in Eqs. (13) and (18), we now study the spatial structure of the plasmon charge density once their initial exponential growth has been cut off by the nonlinear terms of Eq. (11). We focus on a drive and modulation amplitude yielding h just above the instability threshold, such that the unstable region around q^* is infinitesimally thin. The parametric driving is spatially uniform and cannot supply momentum to the system. Therefore,

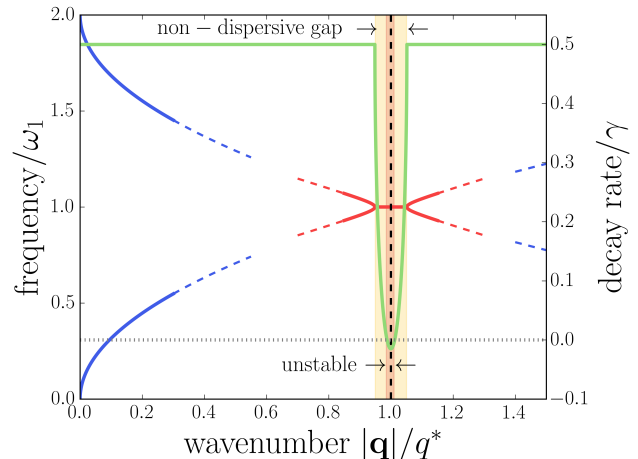


Figure 2. Onset of the plasmon instability induced by modulated Floquet parametric driving with the modulation frequency $2\omega_1$. Red and blue lines show the the quasi-energy dispersion $\text{Re}[\Lambda(q)]$ of parametrically driven plasmons (see Eq. (19) and discussion below). Far away from the critical q^* , 2D plasmons retain the characteristic square-root shape of their dispersion relation (blue lines). The quasi-energy dispersion is invariant with respect to shifts by $2\omega_1$ – the reciprocal lattice constant in frequency space. Near q^* , where $\omega_{\text{pl}}(q^*) \approx \omega_1$ holds, the dispersion is strongly altered by the driving (red lines). A gap which hosts non-dispersive modes opens around q^* (yellow shading). Merging branches of the dispersion at the edges of the non-dispersive gap indicate exceptional points with diverging group velocities. We chose the modulation amplitude h to lie slightly above the instability threshold: damping is negative in a small interval around q^* , leading to an exponential growth of unstable modes (red shading). However, exceptional points and non-dispersive states appear even for subcritical driving strenghts.

plasmons can only be created in pairs with wavevectors $\pm\mathbf{q}^*$, where the star indicates that

$$|\mathbf{q}^*| = q^*. \quad (20)$$

We make the assumption that the final steady state to which the system evolves after the onset of the instability will be some linear combination of the original, linearly unstable modes:

$$\delta\rho_s(t, \mathbf{x}) = \cos(\omega_1 t) \sum_{i=1}^N a^{(i)}(t) \cos(\mathbf{q}^{*(i)} \cdot \mathbf{x}) + \sin(\omega_1 t) \sum_{i=1}^N b^{(i)}(t) \cos(\mathbf{q}^{*(i)} \cdot \mathbf{x}). \quad (21)$$

Here, the wave vectors $\mathbf{q}^{*(i)}$ lie on a circle of radius q^* . The nonlinearities of the system determine the ordering pattern reflected in number of wavevectors N in Eq. (21) and their respective angles [73–75]. Typically a roll ($N = 1$), a square lattice ($N = 2$) or a hexagonal lattice ($N = 3$) is formed, depending on the parameters of the

system. A similar instability appears in parametrically driven shallow water waves, so called Faraday waves [6–8, 73–76]. The Faraday instability has also been reported for cold atom systems [77, 78] and luttinger liquids [79].

For the analysis of pattern formation caused by parametric instabilities, it is sufficient to consider nonlinear terms which project the unstable modes onto themselves [73, 75]. This excludes second order nonlinearities because they give rise to frequency doubling. The third order terms, however, contributes to oscillations at the base frequency ω_1 . Formally, neglecting the second order nonlinearities is equivalent to projecting Eq. (2) onto the restricted subspace of the unstable plane wave modes. Since plasmon modes are longitudinal ($u_{q,j} = \hat{q}_j u_q$) and all wavevectors in Eq. (21) have the length q^* , we can use the linearized continuity equation $\delta\dot{\rho} = -\bar{\rho}\nabla\mathbf{u}$ to approximate

$$u_{s,i} \approx -\partial_i \frac{\delta\rho_s}{q^{*2}\bar{\rho}}. \quad (22)$$

At this point, it is useful to simplify Eq. (11). Rescaling $\delta\rho_s = h^{1/2}\delta\bar{\rho}_s$, we find that to order $\mathcal{O}(h)$, the time dependence of m^* in front of the nonlinear terms can be neglected for $h \ll 1$. Thus, with the approximations described above, for the purpose of finding the modulated pattern of the steady state, Eq. (11) is reduced to

$$\partial_t m^*(t) \partial_t \delta\rho_s + \gamma \bar{m}^* \partial_t \delta\rho_s - \frac{\bar{m}^*}{q^{*4}\bar{\rho}^2} \partial_i \partial_j \delta\rho_s (\partial_i \delta\rho_s) (\partial_j \delta\rho_s) = 0, \quad (23)$$

where $\delta\rho_s$ is given by Eq. (21) and derivatives act on all functions to their right.

In equilibrium the system is rotationally symmetric, and we assume that all standing waves in Eq. (21) have equal amplitudes: $a^{(i)} = a$, $b^{(i)} = b$, for all i and with an arbitrary number of modes N included. This is a common assumption in the analysis of pattern formation due to parametric instabilities [73, 75]. An evaluation of Eq. (23) in which modes lying outside the subspace of unstable modes are neglected leads to amplitude equations

$$\begin{aligned} \dot{a} &= -\alpha b - \frac{1}{2}\gamma a + \beta b(a^2 + b^2) \\ \dot{b} &= -\alpha a - \frac{1}{2}\gamma b - \beta a(a^2 + b^2), \end{aligned} \quad (24)$$

with $\alpha = \omega_1 h/4$ and $\beta = \omega_1 \Gamma_N/32(\bar{\rho})^2$, where $\Gamma_N = 2N - 1$ [80]. For $\gamma = 0$, the Eqs. (24) correspond to the equations of motion arising from the Hamiltonian

$$H(a, b) = \frac{1}{2}\alpha(a^2 - b^2) + \frac{1}{4}\beta(a^4 + b^4) + \frac{1}{2}\beta a^2 b^2. \quad (25)$$

The stable minima of the Hamiltonian (25) are located at:

$$a = 0, \quad b = \pm\sqrt{\frac{\alpha}{\beta}}, \quad (26)$$

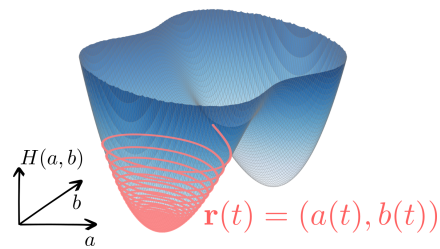


Figure 3. The effective Hamiltonian of Eq. (25) in amplitude space, with the two minima corresponding to symmetry breaking states. The red trajectory is a solution to Eqs. (24) and shows the transition to the crystalline state in the presence of damping.

and their depth is given by $H(\pm\sqrt{\alpha/\beta}, 0) \sim -\Gamma_N^{-1}$. In the presence of weak damping, Eqs. (24) predict that, for any initial condition, the trajectory $r(t) = (a(t), b(t))$ will descend to one of the minima predicted by Eq. (26) (see Fig. 3). The preferred state will be the one with the deepest minimum. Therefore, the optimal configuration is a charge density wave with

$$N = 1 \quad (27)$$

illustrated in Fig. 1.

It should be noted that our analysis of the crystalline state was carried out for an idealized system. Details of an experimental setup, e.g., boundary conditions, or additional nonlinearities could change the effective Hamiltonian of Eq. (25), making a pattern with $N > 1$ more favorable. In any case, our analysis of the instability indicates that the time and length scales of the resulting structures will be given by q^* and ω_1 .

In what follows, we will assume that the system is in the optimal state with $N = 1$.

IV. COLLECTIVE MODES OF THE NON-EQUILIBRIUM STATE

A. Goldstone-like phonons

The crystalline steady state breaks the rotational and translational symmetries of the system. In the following, we show that this symmetry breaking manifests itself in the presence of Goldstone-like phonon modes.

Above, we have found the steady state solution: $\delta\rho = \pm\sqrt{\alpha/\beta} \sin(\omega_1 t) \cos(q^* x)$ (see Eqs. (21), (26)), where for simplicity, we have chosen the x-axis to align with \mathbf{q}^* . The solution remains valid if we shift the phase of the spatial part by φ :

$$\delta\rho = \pm\sqrt{\frac{\alpha}{\beta}} \sin(\omega_1 t) \cos(q^* x + \varphi). \quad (28)$$

If homogeneous and static, the phase shift can always be eliminated by the coordinate transformation $x \rightarrow x -$

φ/q^* . However, if the phase shift is spatially dependent, Eq. (11) will yield conditions on its dynamics. Thus, we investigate the dynamics of $\varphi(t, \mathbf{x})$, such that the $\delta\rho = \pm A \sin(\omega_1 t) \cos[q^* x + \varphi(t, \mathbf{x})]$ remains an approximate solution to Eq. (11). Since a uniform φ has no influence on the dynamics of the system, we expect slow dynamics for a long wavelength spatial dependence of $\varphi(t, \mathbf{x})$, i.e. we expect Goldstone modes.

To proceed, we write

$$\delta\rho = \frac{A}{2} [\sin(\omega_1 t - q^* x - \varphi(t, \mathbf{x})) + \sin(\omega_1 t + q^* x + \varphi(t, \mathbf{x}))], \quad (29)$$

and choose the ansatz

$$\varphi(t, \mathbf{x}) = \varphi_0 e^{-i\Omega t + i\mathbf{Q} \cdot \mathbf{x}} \quad (30)$$

for $\varphi(t, \mathbf{x})$, where

$$\frac{Q}{q^*} \ll 1, \quad \frac{\Omega}{\omega_1} \ll 1. \quad (31)$$

We insert Eq. (29) into Eq. (11) and compare the coefficients in front of the resulting $\sin[\omega_1 t \pm q^* x \pm \varphi(t, \mathbf{x})]$ and $\cos[\omega_1 t \pm q^* x \pm \varphi(t, \mathbf{x})]$ terms in the equations. The equation governing the propagation of the local phase shift $\varphi(t, \mathbf{x})$ follows from the cosine terms. To leading order in $\varphi(t, \mathbf{x})$, Q/q_s and Ω/ω_1 , we find

$$\frac{\partial^2}{\partial t^2} \varphi = \frac{\omega_1^2/q^{*2}}{1-h/2} \left(\left(1 + \frac{5}{2}h\right) \frac{\partial^2}{\partial x^2} \varphi + (1+h) \frac{\partial^2}{\partial y^2} \varphi \right). \quad (32)$$

The equation obtained from comparing the coefficients in front of the sine terms is fulfilled identically to leading order in Ω/ω_1 .

The dispersion in Eqs. (32) describes soft sound-like modes which can be thought of as the phonons of the crystalline state. Their dispersion

$$\Omega_{\pm} \approx \pm \frac{\omega_1}{q^*} \sqrt{\left(1 + \frac{5}{2}h\right) Q_x^2 + (1+h) Q_y^2} \quad (33)$$

is anisotropic and depends on the magnitude of the Floquet modulation h . Interestingly, similar modes have been observed in parametrically driven classical liquids [81].

B. Optical modes

Besides the Goldstone modes of Eq. (32), the symmetry breaking state supports optical modes. These correspond to oscillations of the amplitudes a , b in the Eqs. (24).

To derive the dispersion of the optical modes, we expand the effective Hamiltonian of Eq. (25) around the minimum at $a = 0$, $b = \sqrt{\alpha/\beta}$:

$$H \approx -\frac{\alpha^2}{4\beta} + \alpha (\delta b^2 + \delta a^2). \quad (34)$$

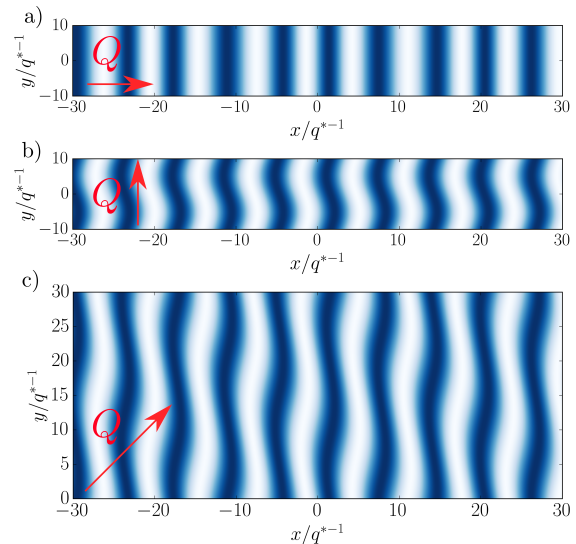


Figure 4. Electron density $\delta\rho$ of Eq. (28) in the presence of the Goldstone-like phonon modes described by Eq. (32). The crystal axis $\hat{\mathbf{q}}^*$ is aligned with the x -axis. The phase $\varphi(t, \mathbf{x})$ propagates in a) x -direction b) y -direction c) in the direction of $(\hat{\mathbf{e}}_x + \hat{\mathbf{e}}_y)/\sqrt{2}$.

Then, Hamilton's equations read

$$\begin{aligned} \delta\dot{b} &= 2\alpha\delta a \\ \delta\dot{a} &= -2\alpha\delta b, \end{aligned} \quad (35)$$

and are solved by a uniform oscillation of the amplitudes with the frequency 2α :

$$\delta\ddot{a} + 4\alpha^2\delta a = 0, \quad (36)$$

with $\alpha = \omega_1 h/4$.

The collective modes of the symmetry broken state described by Eqs. (33) and (36) are one possible experimental signature of the crystalline state. When the dissipation rate γ is included, the modes will obtain a negative imaginary part $\sim -i\gamma$ broadening the resonances.

V. DISCUSSION

Gapped two dimensional Dirac materials are currently an active area of research in material science [82, 83] and promising candidates for Floquet engineering. Recently, ARPES measurements revealed light-induced gaps in black phosphorus [16] in the off-resonant regime considered here. Many interesting features of MFPD, such as exceptional points and non-dispersive states, appear below the critical driving strengths determined by the instability condition $h > 2\gamma/\omega_1$, making them accessible for lasers with relatively low powers. To estimate the power necessary to induce the non-equilibrium crystalline phase, we assume typical values for the parameters of our

system: $E_g = 0.3\text{ eV}$, $\hbar\Omega_F = 0.35\text{ eV}$, $\lambda = 15\text{ eV}\text{\AA}$. Assuming an electron density of $\bar{\rho} = 1.18 \cdot 10^{11}/\text{cm}^{-2}$, such that the chemical potential is close to, but above the resonance, and a plasmon quality factor of $Q = \omega_1/\gamma \approx 10^2$, from the instability condition $\hbar > 2\gamma/\omega_1$, we find the necessary critical amplitude of the electric field to be $\bar{\mathcal{E}} \approx 4 \cdot 10^5\text{ V/m}$ with a modulation amplitude $\delta\bar{\mathcal{E}} = 0.5\bar{\mathcal{E}}$. Thus the laser intensity required to induce the transition to the crystalline state is by a factor of 10^4 smaller than in current solid state Floquet engineering experiments [12–14, 16] and generally within the reach of continuous wave lasers. The critical driving strength is essentially determined by the plasmon Q . While quality factors of $Q \approx 1.5 \cdot 10^2$ have been observed in graphene [84], quality factors of up to $10^3 - 10^4$ are believed to be reachable in principle [84, 85]. Such high quality factors would allow to further reduce the necessary laser intensity, or to realize the crystalline phase in a regime where the Floquet base drive frequency is smaller than the gap, $\hbar\Omega_F < E_g$, and the modulation of the effective mass is smaller at comparable field strengths..

The phenomena presented here can be implemented in two dimensional Dirac systems, such as black phosphorus or TMDs [86]. Another candidate for realizing our ideas is graphene, where light induced gaps have been observed at $\Omega_F = 46\text{ THz}$ [14].

In summary, modulated Floquet parametric driving offers a road to realize new non-equilibrium electron phases with broken translation symmetries in time and space and non-trivial Goldstone modes. Additionally, MFPD opens new possibilities to excite and control THz plasmons by optical or infrared signals. Given the inter-

est in efficient THz technology, the realization of plasmonic parametric amplifiers, time reversal mirrors and other effects predicted for time-varying photonic materials [71, 72, 87] will advance current plasmonic research. A direct observation of exceptional points and non-dispersive regions can be achieved by mapping the plasmon dispersion, e.g., with spectroscopic measurements [88], while the crystalline plasmon phase can be detected via a spectroscopy of the collective Goldstone and optical modes. Scanning potentiometry could be used to measure the periodic density $\delta\rho$ of the crystalline state [89, 90]. The plasmon lattice could also be observed through light or electron scattering experiments, where it would act similarly to a 2D grating. Finally, we note that similar physics could be implemented using other types of collective modes, e.g., magnons.

ACKNOWLEDGMENTS

We acknowledge useful conversations with Dmitri Basov, Gaurav K. Gupta, Amit Kanigel, and Yiming Pan. E.K. and N.L. thank the Helen Diller Quantum Center for financial support. N.L. is grateful for funding from the ISF Quantum Science and Technology (2074/19) and from the Defense Advanced Research Projects Agency through the DRINQS program, grant No. D18AC00025. M. R. is grateful to the University of Washington College of Arts and Sciences and the Kenneth K. Young Memorial Professorship for support.

-
- [1] Andrea Cavalleri, “Photo-induced superconductivity,” *Contemporary Physics* **59**, 31–46 (2018).
 - [2] Daniele Fausti, RI Tobey, Nicky Dean, Stefan Kaiser, A Dienst, Matthias C Hoffmann, S Pyon, T Takayama, H Takagi, and Andrea Cavalleri, “Light-induced superconductivity in a stripe-ordered cuprate,” *science* **331**, 189–191 (2011).
 - [3] Michael Först, RI Tobey, Simon Wall, Hubertus Bromberger, Vikaran Khanna, Adrian L Cavalieri, Y-D Chuang, WS Lee, R Moore, WF Schlotter, *et al.*, “Driving magnetic order in a manganite by ultrafast lattice excitation,” *Physical Review B* **84**, 241104 (2011).
 - [4] Matteo Rini, Ra’anan Tobey, Nicky Dean, Jiro Itatani, Yasuhide Tomioka, Yoshinori Tokura, Robert W Schoenlein, and Andrea Cavalleri, “Control of the electronic phase of a manganite by mode-selective vibrational excitation,” *Nature* **449**, 72–74 (2007).
 - [5] Mark S Rudner and Justin CW Song, “Self-induced berry flux and spontaneous non-equilibrium magnetism,” *Nature Physics* **15**, 1017–1021 (2019).
 - [6] Michael Faraday, “On a peculiar class of acoustical figures; and on certain forms assumed by groups of particles upon vibrating elastic surfaces,” *Philosophical transactions of the Royal Society of London*, 299–340 (1831).
 - [7] Thomas Brooke Benjamin and Fritz Joseph Ursell, “The stability of the plane free surface of a liquid in vertical periodic motion,” *Proceedings of the Royal Society of London. Series A. Mathematical and Physical Sciences* **225**, 505–515 (1954).
 - [8] Krishna Kumar and Laurette S Tuckerman, “Parametric instability of the interface between two fluids,” *Journal of Fluid Mechanics* **279**, 49–68 (1994).
 - [9] Takashi Oka and Hideo Aoki, “Photovoltaic hall effect in graphene,” *Physical Review B* **79**, 081406 (2009).
 - [10] Takuya Kitagawa, Takashi Oka, Arne Brataas, Liang Fu, and Eugene Demler, “Transport properties of nonequilibrium systems under the application of light: Photoinduced quantum hall insulators without landau levels,” *Physical Review B* **84**, 235108 (2011).
 - [11] Netanel H Lindner, Gil Refael, and Victor Galitski, “Floquet topological insulator in semiconductor quantum wells,” *Nature Physics* **7**, 490–495 (2011).
 - [12] YH Wang, Hadar Steinberg, Pablo Jarillo-Herrero, and Nuh Gedik, “Observation of floquet-bloch states on the surface of a topological insulator,” *Science* **342**, 453–457 (2013).
 - [13] Fahad Mahmood, Ching-Kit Chan, Zhanybek Alpichshev, Dillon Gardner, Young Lee, Patrick A Lee, and

- Nuh Gedik, “Selective scattering between floquet–bloch and volkov states in a topological insulator,” *Nature Physics* **12**, 306–310 (2016).
- [14] James W McIver, Benedikt Schulte, F-U Stein, Toru Matsuyama, Gregor Jotzu, Guido Meier, and Andrea Cavigliari, “Light-induced anomalous hall effect in graphene,” *Nature physics* **16**, 38–41 (2020).
- [15] Takuya Kitagawa, Erez Berg, Mark Rudner, and Eugene Demler, “Topological characterization of periodically driven quantum systems,” *Physical Review B* **82**, 235114 (2010).
- [16] Shaohua Zhou, Changhua Bao, Benshu Fan, Hui Zhou, Qixuan Gao, Haoyuan Zhong, Tianyun Lin, Hang Liu, Pu Yu, Peizhe Tang, *et al.*, “Pseudospin-selective floquet band engineering in black phosphorus,” *Nature* **614**, 75–80 (2023).
- [17] Gonzalo Usaj, Pablo Matías Perez-Piskunow, LEF Foa Torres, and Carlos Antonio Balseiro, “Irradiated graphene as a tunable floquet topological insulator,” *Physical Review B* **90**, 115423 (2014).
- [18] Pablo Matías Perez-Piskunow, Gonzalo Usaj, Carlos Antonio Balseiro, and LEF Foa Torres, “Floquet chiral edge states in graphene,” *Physical Review B* **89**, 121401 (2014).
- [19] Takashi Oka and Sota Kitamura, “Floquet engineering of quantum materials,” *Annual Review of Condensed Matter Physics* **10**, 387–408 (2019).
- [20] Or Katz, Gil Refael, and Netanel H Lindner, “Optically induced flat bands in twisted bilayer graphene,” *Physical Review B* **102**, 155123 (2020).
- [21] Iliya Esin, Mark S Rudner, Gil Refael, and Netanel H Lindner, “Quantized transport and steady states of floquet topological insulators,” *Physical Review B* **97**, 245401 (2018).
- [22] Iliya Esin, Mark S Rudner, and Netanel H Lindner, “Floquet metal-to-insulator phase transitions in semiconductor nanowires,” *Science advances* **6**, eaay4922 (2020).
- [23] Iliya Esin, Gaurav Kumar Gupta, Erez Berg, Mark S Rudner, and Netanel H Lindner, “Electronic floquet gyro-liquid crystal,” *Nature communications* **12**, 1–12 (2021).
- [24] Hossein Dehghani, Takashi Oka, and Aditi Mitra, “Out-of-equilibrium electrons and the hall conductance of a floquet topological insulator,” *Physical Review B* **91**, 155422 (2015).
- [25] Maximilian Genske and Achim Rosch, “Floquet-boltzmann equation for periodically driven fermi systems,” *Physical Review A* **92**, 062108 (2015).
- [26] LI Glazman, “Kinetics of electrons and holes in direct-gap semiconductors photo-excited by high-intensity pulses,” *Soviet Physics Semiconductors-USSR* **17**, 494–498 (1983).
- [27] Hossein Dehghani, Takashi Oka, and Aditi Mitra, “Dissipative floquet topological systems,” *Physical Review B* **90**, 195429 (2014).
- [28] MA Sentef, M Claassen, AF Kemper, B Moritz, T Oka, JK Freericks, and TP Devereaux, “Theory of floquet band formation and local pseudospin textures in pump-probe photoemission of graphene,” *Nature communications* **6**, 7047 (2015).
- [29] Ching-Kit Chan, Patrick A Lee, Kenneth S Burch, Jung Hoon Han, and Ying Ran, “When chiral photons meet chiral fermions: photoinduced anomalous hall effects in weyl semimetals,” *Physical review letters* **116**, 026805 (2016).
- [30] Aaron Farrell and T Pereg-Barnea, “Photon-inhibited topological transport in quantum well heterostructures,” *Physical Review Letters* **115**, 106403 (2015).
- [31] Zhenghao Gu, HA Fertig, Daniel P Arovas, and Assa Auerbach, “Floquet spectrum and transport through an irradiated graphene ribbon,” *Physical review letters* **107**, 216601 (2011).
- [32] Hannes Hübener, Michael A Sentef, Umberto De Giovannini, Alexander F Kemper, and Angel Rubio, “Creating stable floquet–weyl semimetals by laser-driving of 3d dirac materials,” *Nature communications* **8**, 13940 (2017).
- [33] Liang Jiang, Takuya Kitagawa, Jason Alicea, AR Akhmerov, David Pekker, Gil Refael, J Ignacio Cirac, Eugene Demler, Mikhail D Lukin, and Peter Zoller, “Majorana fermions in equilibrium and in driven cold-atom quantum wires,” *Physical review letters* **106**, 220402 (2011).
- [34] Dante M Kennes, Niclas Müller, Mikhail Pletyukhov, Clara Weber, Christoph Bruder, Fabian Hassler, Jelena Klinovaja, Daniel Loss, and Herbert Schoeller, “Chiral one-dimensional floquet topological insulators beyond the rotating wave approximation,” *Physical Review B* **100**, 041103 (2019).
- [35] Arijit Kundu and Babak Seradjeh, “Transport signatures of floquet majorana fermions in driven topological superconductors,” *Physical review letters* **111**, 136402 (2013).
- [36] Manisha Thakurathi, Daniel Loss, and Jelena Klinovaja, “Floquet majorana fermions and parafermions in driven rashba nanowires,” *Physical Review B* **95**, 155407 (2017).
- [37] Regine Frank, “Quantum criticality and population trapping of fermions by non-equilibrium lattice modulations,” *New Journal of Physics* **15**, 123030 (2013).
- [38] Alberto Castro, Umberto De Giovannini, Shunsuke A Sato, Hannes Hübener, and Angel Rubio, “Floquet engineering the band structure of materials with optimal control theory,” *Physical Review Research* **4**, 033213 (2022).
- [39] Mark S Rudner and Netanel H Lindner, “Band structure engineering and non-equilibrium dynamics in floquet topological insulators,” *Nature reviews physics* **2**, 229–244 (2020).
- [40] Dominic V Else, Bela Bauer, and Chetan Nayak, “Floquet time crystals,” *Physical review letters* **117**, 090402 (2016).
- [41] Norman Y Yao, Andrew C Potter, I-D Potirniche, and Ashvin Vishwanath, “Discrete time crystals: Rigidity, criticality, and realizations,” *Physical review letters* **118**, 030401 (2017).
- [42] Antonis Kyprianidis, Francisco Machado, William Morong, Patrick Becker, Kate S Collins, Dominic V Else, Lei Feng, Paul W Hess, Chetan Nayak, Guido Pagano, *et al.*, “Observation of a prethermal discrete time crystal,” *Science* **372**, 1192–1196 (2021).
- [43] Jiehang Zhang, Paul W Hess, A Kyprianidis, Petra Becker, A Lee, J Smith, Gaetano Pagano, I-D Potirniche, Andrew C Potter, Ashvin Vishwanath, *et al.*, “Observation of a discrete time crystal,” *Nature* **543**, 217–220 (2017).
- [44] Soonwon Choi, Joonhee Choi, Renate Landig, Georg Kucsko, Hengyun Zhou, Junichi Isoya, Fedor Jelezko, Shinobu Onoda, Hitoshi Sumiya, Vedika Khemani, *et al.*, “Observation of discrete time-crystalline order in a disordered dipolar many-body system,” *Nature* **543**, 221–225

- (2017).
- [45] Muath Natsheh, Andrea Gambassi, and Aditi Mitra, “Critical properties of the prethermal floquet time crystal,” *Physical Review B* **103**, 224311 (2021).
- [46] Achilleas Lazarides, Arnab Das, and Roderich Moessner, “Equilibrium states of generic quantum systems subject to periodic driving,” *Physical Review E* **90**, 012110 (2014).
- [47] Luca D’Alessio and Marcos Rigol, “Long-time behavior of isolated periodically driven interacting lattice systems,” *Physical Review X* **4**, 041048 (2014).
- [48] Marin Bukov, Markus Heyl, David A Huse, and Anatoli Polkovnikov, “Heating and many-body resonances in a periodically driven two-band system,” *Physical Review B* **93**, 155132 (2016).
- [49] Marin Bukov, Luca D’Alessio, and Anatoli Polkovnikov, “Universal high-frequency behavior of periodically driven systems: from dynamical stabilization to floquet engineering,” *Advances in Physics* **64**, 139–226 (2015).
- [50] Dominic V Else, Bela Bauer, and Chetan Nayak, “Prethermal phases of matter protected by time-translation symmetry,” *Physical Review X* **7**, 011026 (2017).
- [51] Takashi Mori, “Floquet prethermalization in periodically driven classical spin systems,” *Physical Review B* **98**, 104303 (2018).
- [52] Martin Reitter, Jakob Näger, Karen Wintersperger, Christoph Sträter, Immanuel Bloch, André Eckardt, and Ulrich Schneider, “Interaction dependent heating and atom loss in a periodically driven optical lattice,” *Physical review letters* **119**, 200402 (2017).
- [53] Kevin Singh, Cora J Fujiwara, Zachary A Geiger, Ethan Q Simmons, Mikhail Lipatov, Alec Cao, Peter Dotti, Shankari V Rajagopal, Ruwan Senaratne, Toshihiko Shimasaki, *et al.*, “Quantifying and controlling prethermal nonergodicity in interacting floquet matter,” *Physical Review X* **9**, 041021 (2019).
- [54] VM Galitsky, SP Goreslavsky, and VF Elesin, “Electric and magnetic properties of a semiconductor in the field of a strong electromagnetic wave,” *SOV PHYS JETP* **30**, 117–122 (1970).
- [55] Tatsuhiko Shirai, Takashi Mori, and Seiji Miyashita, “Condition for emergence of the floquet-gibbs state in periodically driven open systems,” *Physical Review E* **91**, 030101 (2015).
- [56] Karthik I Seetharam, Charles-Edouard Bardyn, Natan H Lindner, Mark S Rudner, and Gil Refael, “Controlled population of floquet-bloch states via coupling to bose and fermi baths,” *Physical Review X* **5**, 041050 (2015).
- [57] Thomas Iadecola, Titus Neupert, and Claudio Chamon, “Occupation of topological floquet bands in open systems,” *Physical Review B* **91**, 235133 (2015).
- [58] Karthik I Seetharam, Charles-Edouard Bardyn, Natan H Lindner, Mark S Rudner, and Gil Refael, “Steady states of interacting floquet insulators,” *Physical Review B* **99**, 014307 (2019).
- [59] Dong E Liu, “Classification of the floquet statistical distribution for time-periodic open systems,” *Physical Review B* **91**, 144301 (2015).
- [60] Dmitry A Abanin, Wojciech De Roeck, and François Huveneers, “Exponentially slow heating in periodically driven many-body systems,” *Physical review letters* **115**, 256803 (2015).
- [61] Adolfo Eguiluz and JJ Quinn, “Hydrodynamic model for surface plasmons in metals and degenerate semiconductors,” *Physical Review B* **14**, 1347 (1976).
- [62] David Pines and Philippe Nozières, *Theory Of Quantum Liquids: Normal Fermi Liquids* (CRC Press, 1989) ISBN 978-0201407747.
- [63] U. Briskot, M. Schütt, I. V. Gornyi, M. Titov, B. N. Narozhny, and A. D. Mirlin, “Collision-dominated non-linear hydrodynamics in graphene,” *Phys. Rev. B* **92**, 115426 (2015).
- [64] D. Forster, *Hydrodynamic Fluctuations, Broken Symmetry, and Correlation Functions* (CRC Press, 2018) ISBN 978-0367091323.
- [65] L. D. Landau and E. M. Lifshits, *Fluid mechanics* (Butterworth-Heinemann, 1987) ISBN 978-0750627672.
- [66] Andrew Lucas and Subir Sachdev, “Memory matrix theory of magnetotransport in strange metals,” *Physical Review B* **91**, 195122 (2015).
- [67] L. D. Landau and E. M. Lifshitz, *Mechanics* (Butterworth-Heinemann, 1976) ISBN 978-0750628969.
- [68] A. Lucas and S. Das Sarma, “Electronic sound modes and plasmons in hydrodynamic two-dimensional metals,” *Phys. Rev. B* **97**, 115449 (2018).
- [69] Egor I Kiselev, “Universal superdiffusive modes in charged two dimensional liquids,” *Physical Review B* **103**, 235116 (2021).
- [70] The Fourier transform of the Coulomb potential is $V(q) = 2\pi/q$ and is responsible for the characteristic $\sim \sqrt{q}$ dispersion of two dimensional plasmons, whereas the pressure term scales as $\sim q$ and will only contribute a small correction.
- [71] Mark Lyubarov, Yaakov Lumer, Alex Dikopoltsev, Eran Lustig, Yonatan Sharabi, and Mordechai Segev, “Amplified emission and lasing in photonic time crystals,” *Science* **377**, 425–428 (2022).
- [72] Emanuele Galiffi, Romain Tirole, Shixiong Yin, Huanan Li, Stefano Vezzoli, Paloma A Huidobro, Mário G Silveirinha, Riccardo Sapienza, Andrea Alù, and JB Pendry, “Photonics of time-varying media,” *Advanced Photonics* **4**, 014002 (2022).
- [73] Peilong Chen and Jorge Vinals, “Amplitude equation and pattern selection in faraday waves,” *Physical Review E* **60**, 559 (1999).
- [74] Peilong Chen and Jorge Vinals, “Pattern selection in faraday waves,” *Physical Review Letters* **79**, 2670 (1997).
- [75] Hanns Walter Müller, “Model equations for two-dimensional quasipatterns,” *Physical Review E* **49**, 1273 (1994).
- [76] W Stuart Edwards and S Fauve, “Patterns and quasipatterns in the faraday experiment,” *Journal of Fluid Mechanics* **278**, 123–148 (1994).
- [77] Andrea Di Carli, Robbie Cruickshank, Matthew Mitchell, Arthur La Rooij, Stefan Kuhr, Charles E Creffield, and Elmar Haller, “Instabilities of interacting matter waves in optical lattices with floquet driving,” *arXiv preprint arXiv:2303.06092* (2023).
- [78] Nathan Dupont, Lucas Gabardos, Floriane Arrouas, Gabriel Chatelain, Maxime Arnal, Juliette Billy, Peter Schlagheck, Bruno Peaudecerf, and David Guéry-Odelin, “Emergence of a tunable crystalline order in a floquet-bloch system from a parametric instability,” *arXiv preprint arXiv:2212.10890* (2022).
- [79] Serena Fazzini, Piotr Chudzinski, Christoph Dauer, Imke Schneider, and Sebastian Eggert, “Nonequilibrium flo-

- quet steady states of time-periodic driven luttinger liquids,” *Physical Review Letters* **126**, 243401 (2021).
- [80] Eq. (24) is the nonlinear generalization of the slowly varying mode approximation of Eq. (15). In deriving it, we again neglected higher order derivatives of the amplitudes, as well as terms of the order $\dot{a}/(\omega_1 a)$, $\dot{b}/(\omega_1 b)$, because for an h just above the instability threshold, the dynamics of $a(t)$, $b(t)$ is slow compared to the oscillation at frequency ω_1 .
- [81] L Domino, M Tarpin, Sylvain Patinet, and A Eddi, “Faraday wave lattice as an elastic metamaterial,” *Physical Review E* **93**, 050202 (2016).
- [82] A Chaves, Javad G Azadani, Hussain Alsalman, DR Da Costa, R Frisenda, AJ Chaves, Seung Hyun Song, Young Duck Kim, Daowei He, Jiadong Zhou, *et al.*, “Bandgap engineering of two-dimensional semiconductor materials,” *npj 2D Materials and Applications* **4**, 1–21 (2020).
- [83] AJ Chaves, RM Ribeiro, T Frederico, and NMR Peres, “Excitonic effects in the optical properties of 2d materials: an equation of motion approach,” *2D Materials* **4**, 025086 (2017).
- [84] GuangXin Ni, d AS McLeod, Zhiyuan Sun, Lei Wang, Lin Xiong, KW Post, SS Sunku, B-Y Jiang, James Hone, Cory R Dean, *et al.*, “Fundamental limits to graphene plasmonics,” *Nature* **557**, 530–533 (2018).
- [85] Alessandro Principi, Giovanni Vignale, Matteo Carrega, and Marco Polini, “Intrinsic lifetime of dirac plasmons in graphene,” *Physical Review B* **88**, 195405 (2013).
- [86] Sajedeh Manzeli, Dmitry Ovchinnikov, Diego Pasquier, Oleg V Yazyev, and Andras Kis, “2d transition metal dichalcogenides,” *Nature Reviews Materials* **2**, 1–15 (2017).
- [87] Eran Lustig, Yonatan Sharabi, and Mordechai Segev, “Topological aspects of photonic time crystals,” *Optica* **5**, 1390–1395 (2018).
- [88] SY Shin, ND Kim, JG Kim, KS Kim, DY Noh, Kwang S Kim, and JW Chung, “Control of the π plasmon in a single layer graphene by charge doping,” *Applied Physics Letters* **99**, 082110 (2011).
- [89] Zachary J Krebs, Wyatt A Behn, Songci Li, Keenan J Smith, Kenji Watanabe, Takashi Taniguchi, Alex Levchenko, and Victor W Brar, “Imaging the breaking of electrostatic dams in graphene for ballistic and viscous fluids,” *Science* **379**, 671–676 (2023).
- [90] Rolf Möller, Uwe Albrecht, Johannes Boneberg, Berndt Koslowski, Paul Leiderer, and Klaus Dransfeld, “Detection of surface plasmons by scanning tunneling microscopy,” *Journal of Vacuum Science & Technology B: Microelectronics and Nanometer Structures Processing, Measurement, and Phenomena* **9**, 506–509 (1991).